Inorganic Chemistry

Article

pubs.acs.org/IC

A Ru(II) Bis-terpyridine-like Complex that Catalyzes Water Oxidation: The Influence of Steric Strain

Nattawut Kaveevivitchai, Lars Kohler, Ruifa Zong, Maya El Ojaimi, Nirja Mehta, and Randolph P. Thummel*

Department of Chemistry, 110 Fleming Building, University of Houston, Houston, Texas 77204-5003, United States

Supporting Information

ABSTRACT: The complexation of 2,9-dicarboxy-1,10-phenanthroline (DPA) with [Ru(tpy)Cl_3] (tpy = 2,2′;6,2″-terpyridine) provides a six-coordinate species in which one carboxyl group of DPA is not bound to the Ru(II) center. A more soluble tri-*t*-butyl tpy analogue is also prepared. Upon oxidation, neither species shows evidence for intramolecular trapping of a seven-coordinate intermediate. The role of the tpy ligand is revealed by the preparation of [Ru(tpy)(phenq)]$^{2+}$ (phenq = 2-(quinol-8′-yl)-1,10-phenanthroline) that behaves as an active water oxidation catalyst (TON = 334). This activity is explained by the expanded coordination geometry of the phenq ligand that can form a six-membered chelate ring that better accommodates the linear arrangement of axial ligands required for optimal pentagonal bipyramid geometry. When a 1,8-naphthyidine ring is substituted for each of the two peripheral pyridine rings on tpy, increased crowding in the vicinity of the metal center impedes acquisition of the prerequisite reaction geometry.

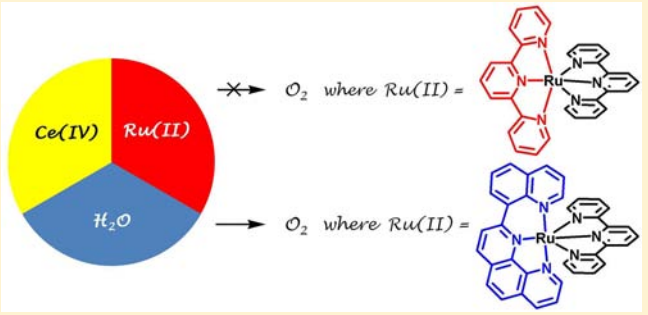

The concept of artificial photosynthesis involves the cooperative interaction of chemistry and sunlight to drive some of the fundamental processes of life. Considerable recent attention has been focused on the use of a light driven catalyst to decompose water into its elements.[1] The two half-reactions in this process are the reduction of protons and the oxidation of hydroxide. The latter reaction is considered more challenging since it involves the transfer of four electrons and the combination of two water molecules. Therefore, the development of an efficient and stable catalyst for water oxidation has become an important target.[2]

Recently, a variety of transition metal complexes have been studied as catalysts for the oxidation of water. Among the most effective of these catalysts are ones based on Ru(II).[3] We and others have reported on three types of mononuclear Ru(II) catalysts involving polypyridine ligands (**1**−**3**).[4] Catalysts of types **1** and **2** contain a water bound to the Ru(II) center and thus mechanistic concerns center around the oxidation of Ru−OH_2 to the Ru=O species followed by attack of H_2O at the electrophilic oxo group to provide a peroxy intermediate that then decomposes to afford O=O and two protons. Considerable careful study has been devoted to the intimate understanding of the mechanism of this overall oxidation process.[5]

For the type **3** catalyst, prevailing evidence suggests that all the pyridine rings remain bonded to the metal center throughout the catalytic process. In an earlier report, we have suggested that such a species might expand its coordination sphere to seven in order to accommodate a metal-bonded

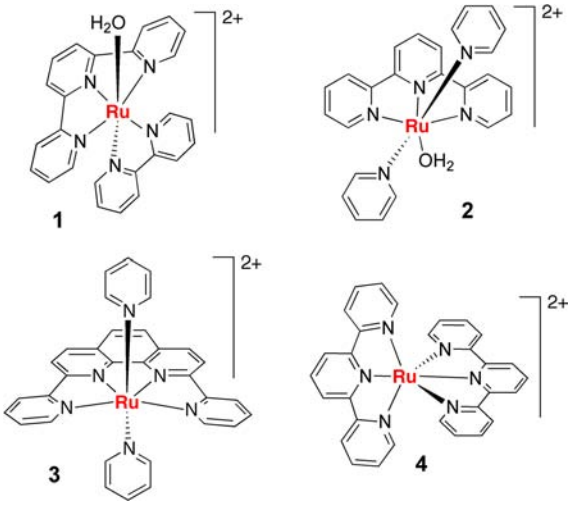

water.[6] This attack by water would be favorable based on a combination of steric and electronic factors. After oxidation from Ru(II) to Ru(IV) the metal center would be electron deficient (16 e−) and thus sufficiently electrophilic to be attacked by water. Also the exterior N−Ru−N angle in the equatorial plane of the tetradentate ligand is 125.6°, and this angle can be readily bisected by a water molecule attacking the Ru(IV) center to restore an 18 electron count.

Received: June 27, 2013
Published: August 29, 2013

   dx.doi.org/10.1021/ic4016383 | *Inorg. Chem.* 2013, 52, 10615−10622

The strain inherent in the tetradentate coordination of the 2,9-di(pyrid-2′-yl)-1,10-phenanthroline (dpp) ligand is an important factor in dictating the reactivity of **3**. A less strained analogue of complex **3** does not show nearly the same reactivity, while related complexes involving derivatives of dpp or different substituted pyridines as axial ligands all show activity in water oxidation. Our observations have been amplified by similar observations from Sun and co-workers regarding the tetradentate ligand 2,9-dicarboxy-1,10-phenanthroline.[7] A complex of this ligand with Ru(II) and two axial picoline ligands is an efficient water oxidation catalyst, and the suspected water-bound seven coordinate intermediate has been verified by an X-ray crystal structure.[8]

In addition, we have made the curious observation that the iodo analogue of complex **2**, having iodide in place of water, was more reactive than the parent aqua-complex.[4b] This observation implies that the iodide ligand might not initially be replaced by water suggesting the possibility of a seven-coordinate intermediate. It should also be noted that for the systems in which expansion of the coordination sphere is being suggested, we always observe a significant induction period of about 1−10 min prior to the onset of oxygen evolution.

The observation that catalysts **1**−**3** all involve a tridentate (2,2′; 6′,2″-terpyridine, tpy) or tetradentate (dpp) ligand implies that steric strain might play an important role in the activity of these systems. This strain would be relieved to some extent by expanding the Ru coordination sphere to seven. The question thus comes to mind as to why $[Ru(tpy)_2]^{2+}$ (**4**) is *not* an effective catalyst.

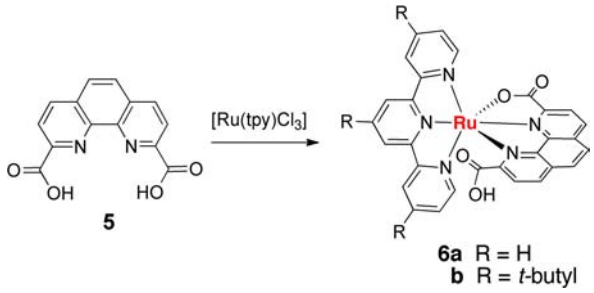

To give some insight into the geometry that might be required to achieve the heptacoordinate species that is being invoked in the initial activation of catalysts such as **3**, we focused our attention on a hexacoordinate system containing a pendant uncomplexed carboxy group that was held close to the metal center. We prepared the complexes **6a** and **6b** from the reaction of 1,10-phenanthroline-2,9-dicarboxylic acid (**5**) with the appropriate $[Ru(NNN)Cl_3]$ reagent. The complexes were characterized by their ^{1}H NMR spectra that, most importantly, showed six equal intensity signals for the six nonequivalent phenanthroline protons, indicating asymmetry and hence tridentate coordination involving only one carboxy group. The tpy complex **6a** showed rather poor solubility in organic solvents, while the 4,4′,4″-tri-*t*-butyl-tpy (tbtpy) analogue **6b** was much more soluble. The downfield region of the NMR spectrum of **6a** is shown in Figure 1 where the three pairs of doublets for the phenanthroline protons are clearly evident along with six signals, five of which integrate for two protons, due to the tpy ligand. For **6b** the *t*-butyl groups showed a 9 proton singlet at 1.73 ppm and an 18 proton singlet at 1.33 ppm.

To verify the coordination geometry, an X-ray crystal structure was obtained for **6a**. An ORTEP plot of the complex

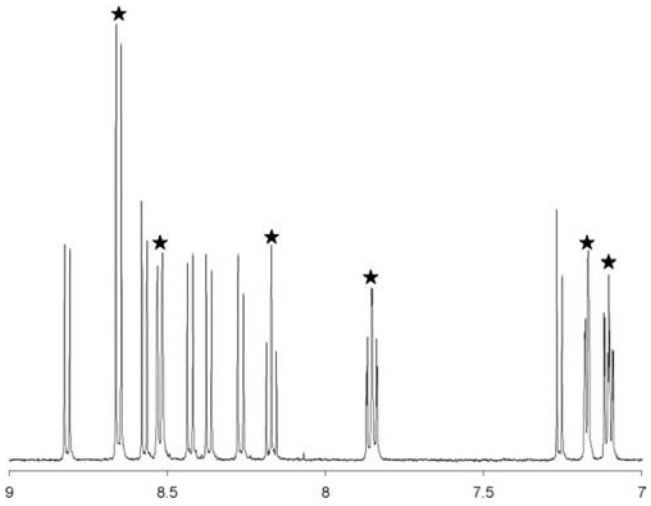

Figure 1. ^{1}H NMR spectrum of **6a** in CD_3OD; tpy protons are starred.

is shown in Figure 2, and selected geometric parameters are listed in Table 1. The Ru−N bonds lengths for the Ru(tpy)

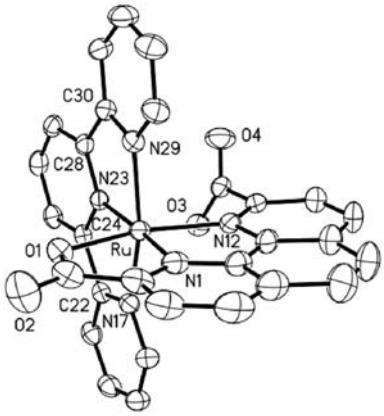

Figure 2. View of **6a** showing the atom numbering scheme for key atoms. Thermal ellipsoids are 40% equiprobability envelopes, with H atoms omitted.

residue are normal with the peripheral bonds being 2.06−2.07 Å and the internal bond being somewhat shorter at 1.97 Å. The three pyridine rings of tpy are slightly noncoplanar with dihedral angles around the interpyridine bonds being 3.5−8.0°. Most importantly, the N29−Ru−N17 angle is 158.3°, considerably less than the 180° demanded by ideal octahedral coordination. The dicarboxyphen coordinates as a tridentate ligand with the unbound carboxy group held relatively close to the metal center. The Ru−O3 distance is 3.63 Å, making this oxygen well poised to attack the oxidized metal center. The tpy ligand is pushed away from this carboxy group so that the angle N23−Ru−O1 (96.5°) is considerably less than N23−Ru−N12 (106.8°), facilitating attack by the unbound carboxy group on the Ru center.

We attempted to promote this attack by treating the complex with Ce(IV) to oxidize the metal center, making it more electrophilic. We were unable to find any evidence for binding of the second carboxy group to provide a seven-coordinate species. We also examined the cyclic voltammetry of **6b**, which, due to the tri-*t*-butyltpy, was more soluble in solvents such as dichloromethane and acetonitrile than **6a**. Figure 3 reveals good

dx.doi.org/10.1021/ic4016383 | *Inorg. Chem.* 2013, 52, 10615−10622

Table 1. Selected Geometric Parameters for 6a and 8

6a		8	
	Bond Lengths (Å)		
Ru−N17	2.0699(19)	Ru−N25	2.072(4)
Ru−N23	1.9744(18)	Ru−N31	1.978(5)
Ru−N29	2.057(2)	Ru−N37	2.072(3)
Ru−N1	1.969(2)	Ru−N1	2.065(4)
Ru−N12	2.109(2)	Ru−N12	2.065(5)
Ru−O1	2.1194(17)	Ru−N23	2.097(6)
Ru−O2	4.118		
Ru−O3	3.628		
Ru−O4	4.238		
	Bond Angles (deg)		
N23−Ru−N29	79.38(8)	N25−Ru−N31	79.73(17)
N23−Ru−N17	78.89(7)	N31−Ru−N37	79.39(18)
N29−Ru−N17	158.26(8)	N25−Ru−N37	159.09(16)
N1−Ru−N17	103.12(8)	N1−Ru−N12	80.9(3)
N1−Ru−N29	98.46(8)	N12−Ru−N23	89.9(2)
N1−Ru−N23	173.35(8)	N1−Ru−N23	170.3(3)
N1−Ru−N12	79.52(9)	N12−Ru−N31	172.43(18)
N23−Ru−N12	106.77(8)	N12−Ru−N25	100.88(19)
N29−Ru−N12	92.08(8)	N12−Ru−N37	99.9(2)
N17−Ru−N12	94.33(8)	N23−Ru−N31	97.68(18)
N1−Ru−O1	77.24(8)	N23−Ru−N25	91.9(4)
N23−Ru−O1	96.45(7)	N23−Ru−N37	89.9(4)
N29−Ru−O1	90.85(7)	N1−Ru−N31	91.5(3)
N17−Ru−O1	91.38(7)	N1−Ru−N37	88.95(19)
N12−Ru−O1	156.75(8)	N1−Ru−N25	92.6(2)
	Dihedral Angles (deg)		
C31−C30−C28−N23	174.11	N25−C23−C32−C33	−177.0(5)
N23−C28−C30−N29	−5.26	N25−C30−C32−N31	1.4(6)
C27−C28−C30−N29	172.67	C29−C30−C32−N31	−179.1(4)
C31−C30−C28−C27	−7.96	C29−C30−C32−C33	2.4(7)
C21−C22−C24−N23	−177.68	C35−C36−C38−N37	176.2(4)
N23−C24−C22−N17	3.47	C35−C36−C38−C39	−4.9(7)
N17−C22−C24−C25	−175.11	N31−C36−C38−C39	175.3(4)
C25−C24−C22−C21	3.74	N31−C36−C38−N37	−3.6(5)
		C10−C11−C15−C24	−155.3(9)
		C10−C11−C15−C16	20.6(9)
		N12−C11−C15−C16	−159.8(6)
		N12−C11−C15−C24	24.3(11)

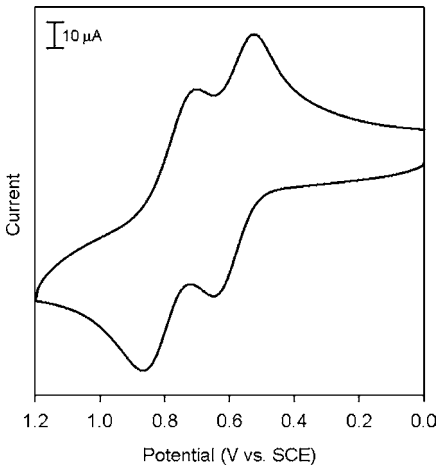

Figure 3. Cyclic voltammogram of **6b** in CH_2Cl_2 (scan rate = 100 mV/s).

quasi-reversible behavior for this complex which would not be expected if carboxylate attack was intercepting the Ru(IV) state. At first glance, this result seems inconsistent with a report by Sun and co-workers in which a very similar Ru(II) complex of 2,9-dicarboxyphen does go to seven-coordinate upon oxidation.[8] The Sun system has two molecules of 4-picoline as the axial ligands. These axial ligands are able to easily align themselves in the linear fashion required for optimal pentagonal bipyramid geometry. For **6a** and **6b** the tpy ligand cannot arrange itself in a similar fashion, significantly increasing the barrier to heptacoordination. This geometric constraint may also explain the failure of **4**, **6a**, or **6b** to act as a water oxidation catalyst.

Similar ligand field strain effects have been invoked to explain the short excited state lifetime for $[Ru(tpy)_2]^{2+}$ and related complexes.[9] In earlier work, we have addressed this problem by relieving strain by increasing the ring size of the two fused tridentate chelate rings from five−five to five−six. This geometric change was accomplished by substituting the ligand phenq (**7**) for tpy with the result that the lifetime at 298 K for

dx.doi.org/10.1021/ic4016383 | Inorg. Chem. 2013, 52, 10615−10622

$[Ru(7)_2]^{2+}$ increased to 810 ns from the value of 0.25 ns observed for $[Ru(tpy)_2]^{2+}$.[10] We decided to use the same geometric approach in an attempt to increase the catalytic activity of $[Ru(tpy)_2]^{2+}$. The phenq was prepared as described previously[11] and then treated with $RuCl_3$-$3H_2O$ to provide the reagent $[Ru(phenq)Cl_3]$ in nearly quantitative yield. Subsequent reaction with tpy provided the heteroleptic complex $[Ru(phenq)(tpy)]^{2+}$ (**8**) in 90% yield. In a similar fashion, the tridentate ligand 4-*t*-butyl-2,6-di(1′,8′-naphthyrid-2′-yl)pyridine (dinappy) was treated with $[Ru(phenq)Cl_3]$ to provide the complex **9** in 22% yield.

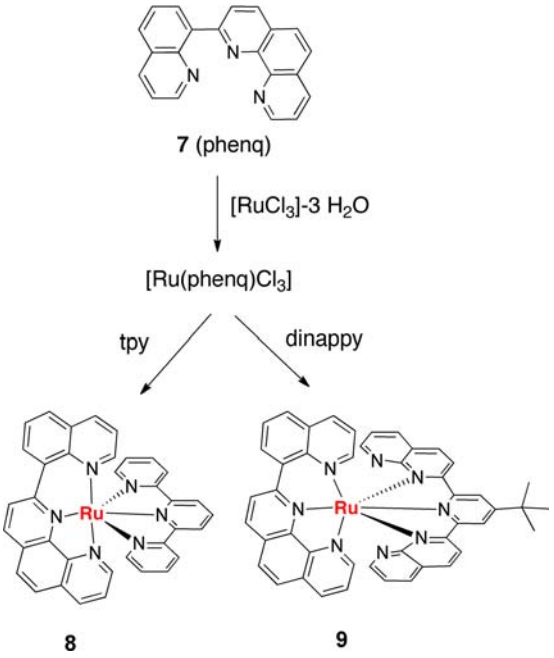

The electronic absorption data and half-wave oxidation and reduction potentials for the complexes under discussion are summarized in Table 2. Complexes **6a** and **6b** show nearly identical absorption spectra, which suggests that the incorporation of three *t*-butyl groups on the tpy ligand does not affect the electronic properties of the complex (Figure S4, Supporting Information). In comparing $[Ru(phenq)(tpy)]^{2+}$ to $[Ru(tpy)_2]^{2+}$, we see that three of the absorptions are red-shifted by 5−10 nm and decrease somewhat in intensity. An additional peak at 352 nm also appears for $[Ru(phenq)(tpy)]^{2+}$. The absorption spectrum for the dinappy complex **9** is red-shifted, and the band at 638 nm is typical for a metal-to-ligand charge transfer from Ru to the more electronegative 1,8-naphthyridyl moiety (Figure S5, Supporting Information).

Because of the poor solubility of **6a** in acetonitrile, we instead measured the half-wave redox potentials for **6b** which was freely soluble in acetonitrile and dichloromethane. In the latter solvent, two quasi-reversible oxidation waves were observed at 0.59 and 0.78 V (Figure 3). A clear reduction wave was not observed. Both complexes **8** and **9** show reversible behavior with the oxidation potential becoming less positive and the reduction potential becoming more positive along the series **4**, **8**, **9**.

In order to understand better the coordination geometry of the phenq ligand bound to Ru(II), we carried out a single crystal X-ray analysis of complex **8**. Figure 4 shows an ORTEP

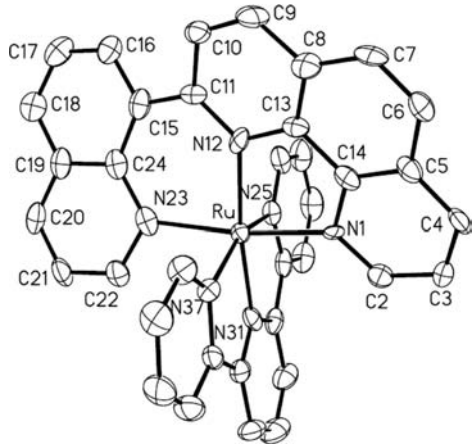

Figure 4. View of **8** showing the atom numbering scheme for key atoms. Thermal ellipsoids are 40% equiprobability envelopes, with H atoms omitted.

plot of the cation of **8**, and Table 1 lists some of the important geometric parameters. Focusing first on the Ru(tpy) portion of the complex, we find that it closely resembles the identical substructure in complex **6a**. The outer two Ru−N bonds are about 2.06−2.07 Å, and the central Ru−N bond length is 1.97 Å. The N−Ru−N angles containing the tpy ligand are also very similar between the two complexes, and the critical N25−Ru−N37 angle of **8** is 159.1°, which is considerably less than the 180° required for optimal octahedral coordination. We find the dihedral angles around the interpyridine bonds of the tpy ligand in **8** to be about 2−4°. These same dihedral angles are slightly larger in **6a** due to the congestion caused by the unbound carboxyl group held close to the metal binding site.

The binding geometry of the phenq ligand in **8** is considerably different from the tpy ligand. The phen portion has identical Ru−N bond lengths (2.065 Å) and a N1−Ru−N12 bond angle of 80.9° that is very close to the N−Ru−N angles of the Ru(tpy) substructure. The Ru−N23 bond to the quinoline moiety is the longest Ru−N bond at 2.10 Å. The six-membered chelate ring opens up the N12−Ru−N23 angle to

Table 2. Electronic Absorption[a] and Electrochemical Potential Data[b] for Ru(II) Complexes

complex	λ_{max}/nm (log ε/M^{-1} cm^{-1})	$E_{1/2}^{ox}$ (ΔE)	$E_{1/2}^{red}$ (ΔE)
4 $[Ru(tpy)_2]^{2+}$	270(4.64), 308(4.85), 475(4.22)	1.28	−1.27
6a	3.14(4.66), 495(4.27)	*c*	*c*
6b	3.13(4.62), 497(4.24)	0.59 (122), 0.78 (163)[d]	*e*
8	280(4.44), 312(4.58), 352(4.31), 480(3.97)	1.18 (82)	−1.18 (83)
9	351 (4.61), 369 (4.39, sh), 502 (3.96), 638 (3.37), 706 (2.96, sh)	1.11 (75)	−0.93 (75), −1.29 (80), −1.68 (82)

[a]Measured in CH_3CN (5.0×10^{-5} M) at 20 °C. [b]Measured with a glassy carbon electrode at 100 mV/s in CH_3CN containing 0.1 M NBu_4PF_6 and $E_{1/2}$ reported in volts relative to SCE; $E_{1/2}$ = (Epa + Epc)/2 in volts, and ΔE = (Epa − Epc) in mV. [c]Poor solubility in CH_3CN. [d]Dichloromethane. [e]No clear reduction wave.

dx.doi.org/10.1021/ic4016383 | *Inorg. Chem.* 2013, 52, 10615−10622

an almost perfect octahedral angle of 89.9°. The N1−Ru−N23 angle of 170.3° is still not completely linear but apparently large enough to make a significant difference in activity. Not unexpectedly, the large dihedral angle of about 22.4° around the phen-quinoline bond reflects the distortion associated with the six-membered chelate ring.

The complexes under consideration were then evaluated for their activity as water oxidation catalysts. The complex in 50 μL of acetonitrile was introduced into a solution containing 5000 equiv of ceric ammonium nitrate that served as a sacrificial oxidant. The initial rate of oxygen evolution was measured by a Clark electrode immersed in the solution, and the turnover number (TON) for active catalysts was measured by GC after a 24 h reaction. Only complex **8** was active with an initial rate constant of 7.4×10^{-3} s^{-1} and a TON = 334. By varying the concentration of **8** from 20 to 160 μM, we were also able to determine that the reaction was first order in catalyst (Figure S6, Supporting Information). We were unable to recover **8** or its decomposition product after reaction. The final pH was measured as 0.7.

The inactivity of **6a** and **6b** as water oxidation catalysts is not surprising. The unbound carboxyl group in these complexes either blocks attack of water on the metal center or could potentially compete for attack. However, our efforts to detect this competing behavior were unsuccessful. As stated earlier, there may also be geometric constraints that inhibit conversion to the pentagonal bipyramid geometry that is required for heptacoordination. This geometric argument would explain the inactivity of $[Ru(tpy)_2]^{2+}$ (**4**) as a catalyst. However, when we substitute phenq for a tpy in **4**, we allow a more linear arrangement of N−Ru−N for the phenq ligand occupying the two axial sites.

We examined the cyclic voltammetry of $[Ru(tpy)_2]^{2+}$ (**4**) and $[Ru(phenq)(tpy)]^{2+}$ (**8**) in aqueous solution at pH = 7 as further evidence of the different chemistry that occurs as one observes the Ru II/III couple. Figure 5 shows this oxidation wave as a function of varying scan rate for the complex **4**. As the scan rate is decreased from 400 to 25 mV/s, the half-wave potential remains essentially unchanged, and the difference between the cathodic and anodic waves also remains approximately constant, indicating good reversible behavior. For complex **8**, however, under the same conditions, the oxidation potential increases from 0.96 to 1.05 V with decreasing scan rate, and the wave eventually becomes irreversible (Figure 6). The irreversible behavior of **8** is likely due to attack by water at the oxidized metal center, a process that is much less likely for oxidized **4**.

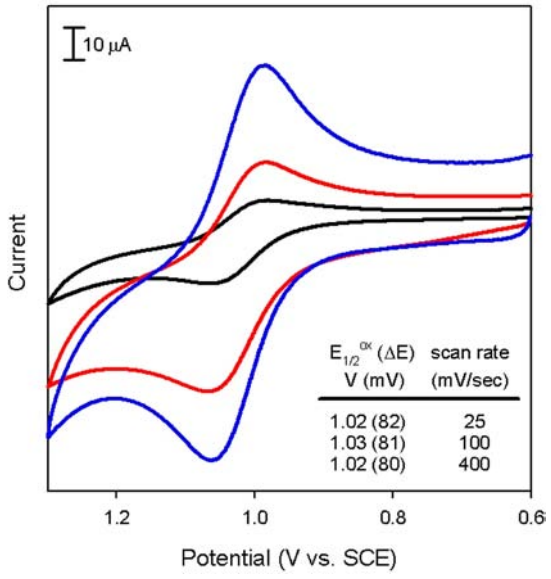

Figure 5. Cyclic voltammograms for $[Ru(tpy)_2]Cl_2$ (2×10^{-3} M) in phosphate buffer (0.2 M; pH 7) at 25 mV/s (black), 100 mV/s (red), and 400 mV/s (blue).

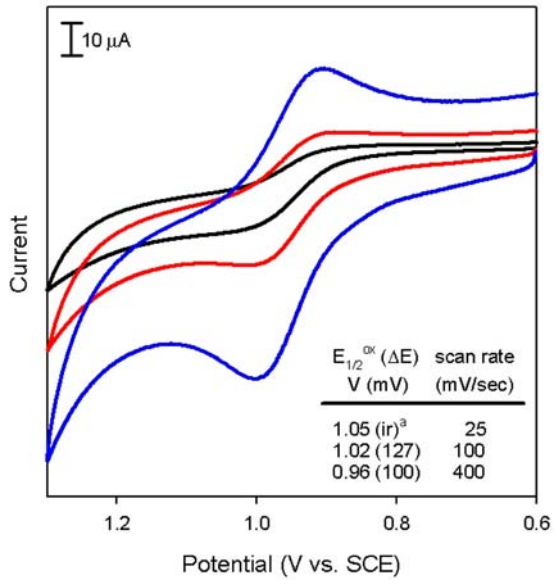

Figure 6. Cyclic voltammograms for $[8]Cl_2$ (2×10^{-3} M) in phosphate buffer (0.2 M; pH 7) at 25 mV/s (black), 100 mV/s (red), and 400 mV/s (blue). [a]For the anodic wave.

The complex **9** is similar to **8** with a 4′-*t*-butyl group and two fused pyrido-rings on the tpy ligand. The two peripheral 1,8-naphthyridyl rings create congestion in the vicinity of the metal center that may impede attack of the water molecule and also cause crowding with the phenq ligand as the coordination geometry increases.

From this study and our previous observations regarding Ru(II) complexes with tridentate and tetradentate ligands, it appears that two important steric requirements must be met for the system to be active as a water oxidation catalyst. Both steric requirements are consistent with water attack in the equatorial plane to form a well organized seven-coordinate intermediate. First, there must be sufficient angle strain due to tridentate or tetradentate coordination in the equatorial plane to promote water to attack in this plane and thereby reduce the angle strain. Second, the axial ligands must be able to achieve a nearly linear arrangement as demanded by the formation of a heptacoordinate pentagonal bipyramid. When terpyridine serves as the axial ligand, it cannot assume this nearly linear geometry, and hence formation of the prerequisite 7-coordinate geometry is not possible. Future studies will explore the mechanistic implications of these steric requirements and will use this knowledge along with relevant electronic effects to design more active and robust water oxidation catalysts.

■ EXPERIMENTAL SECTION

The ^{1}H NMR were recorded at room temperature on a JEOL ECX-400 spectrometer at 400 MHz or on a JEOL ECA-500 spectrometer at

dx.doi.org/10.1021/ic4016383 | *Inorg. Chem.* 2013, 52, 10615−10622

500 MHz. Chemical shifts are referenced to the residual solvent peak and were reported in parts per million (ppm) and the J values are ±0.5 Hz. Electronic absorption spectra were recorded with a VARIAN Cary-50 Bio spectrophotometer and were corrected for the background spectrum of the solvent. Cyclic voltammetry (CV) experiments were performed at room temperature in a one-compartment cell equipped with a glassy carbon working electrode, a saturated calomel reference electrode (SCE), and a platinum wire as the auxiliary electrode in CH_3CN containing (n-butyl)$_4$N(PF_6) (0.1 M) at a scan rate of 100 mV s^{-1}. Mass spectra were obtained on a Voyager-DE-STR MALDI-TOF mass spectrometer using α-cyano-4-hydroxycinnamic acid as matrix.

All reagents and solvents were purchased from commercial sources and were used as received except 1,10-phenanthroline-2,9-dicarboxylic acid (**5**, DPA)[12] and [Ru(tpy)Cl_3][13] that were prepared according to published procedures. The ligand 2-(quinol-8′-yl)-1,10-phenanthroline (phenq) was prepared according to a reported procedure,[11] and [Ru(phenq)Cl_3] was prepared by an adaptation of a reported procedure.[13]

Complex 6a. A mixture of **5** (DPA, 60.9 mg, 0.227 mmol) and [Ru(tpy)Cl_3] (100 mg, 0.227 mmol) in EtOH/H_2O (4:1) in the presence of triethylamine (TEA, 0.3 mL) was refluxed for 2 h. The solvent was evaporated, and the residue was suspended in water and then filtered to remove insolubles. The filtrate was concentrated, and the remaining solid was suspended in CH_3CN (50 mL). After sonication for 10 min, the product was filtered and washed with CH_3CN. Complex **6a** was completely insoluble in CH_3CN and isolated as a red solid (121 mg, 89%): ^{1}H NMR (CD_3OD): δ 8.82 (d, 1H, J = 8.2 Hz, H_{PDA}), 8.65 (d, 2H, J = 8.2 Hz, H_{tpy}), 8.58 (d, 1H, J = 8.2 Hz, H_{PDA}), 8.52 (d, 2H, J = 8.3 Hz, H_{tpy}), 8.43 (d, 1H, J = 8.2 Hz, H_{PDA}), 8.37 (d, 1H, J = 8.2 Hz, H_{PDA}), 8.27 (d, 1H, J = 8.2 Hz, H_{PDA}), 8.18 (t, 1H, J = 8.2 Hz, H_{tpy}), 7.86 (dt, 2H, J = 8.2, 4.0 Hz, H_{tpy}), 7.25 (d, 1H, J = 8.2 Hz, H_{PDA}), 7.17 (dd, 1H, J = 5.2 Hz, 0.9 H_{tpy}), 7.10 (dt, 4H, J = 6.4 Hz, 0.9 H_{tpy}); MS (MALDI-TOF): m/z 602.35 $[M + H]^+$, 558.34 $[M + H - CO_2]^+$.

Complex 6b. In the manner described above for **6a**, a mixture of **5** (DPA, 22.0 mg, 0.082 mmol) and [Ru(tbtpy)Cl_3] (50 mg, 0.082 mmol) in EtOH/H_2O (4:1) in the presence of TEA (0.3 mL) was refluxed for 2 h. The solvent was evaporated. The residue was dissolved in CH_2Cl_2, washed 2 times with water, and concentrated. Recrystallization from CH_2Cl_2/hexane afforded **6b** as a red solid (61 mg, 97%): ^{1}H NMR (CD_3OD): δ 8.75 (d, 1H, J = 8.5 Hz, H_{PDA}), 8.73 (s, 2H, H_{tbtpy}), 8.56 (d, 2H, J = 1.8 Hz, H_{tbtpy}), 8.53 (d, 1H, J = 8.4 Hz, H_{PDA}), 8.40 (d, 1H, J = 8.8 Hz, H_{PDA}), 8.34 (d, 1H, J = 8.0 Hz, H_{PDA}), 8.25 (d, 1H, J = 9.1 Hz, H_{PDA}), 7.27 (d, 1H, J = 8.4 Hz, H_{PDA}), 7.10 (dd, 2H, J = 6.2, 42.2 Hz, H_{tbtpy}), 6.99 (d, 2H, J = 5.4 Hz, H_{tbtpy}) 1.72 (s, 9H, t-Bu), 1.33 (s, 18H, t-Bu).

[Ru(phenq)Cl$_3$]. $RuCl_3 \cdot 3H_2O$ (261.5 mg, 1.00 mmol) and 2-(quinol-8′-yl)-1,10-phenanthroline (phenq, 307.4 mg, 1.00 mmol) were suspended in ethanol (50 mL), and the reaction was refluxed for 5 h. After the mixture was cooled to room temperature, the precipitate was filtered, washed with ethanol, and dried. The [Ru(phenq)Cl_3] was isolated as a dark black solid (508 mg, 99%) and used without further purification.

[Ru(phenq)(tpy)](PF$_6$)$_2$ (8). A mixture of [Ru(phenq)Cl_3] (20 mg, 0.045 mmol) and tpy (11 mg, 0.049 mmol) in EtOH/H_2O (3:1, 20 mL) in the presence of TEA (0.3 mL) was heated at reflux overnight. After the volume was reduced, NH_4PF_6 (100 mg) was added, and the precipitate was collected, washed with water, and dried. Chromatography on alumina, eluting with CH_3CN/acetone (1:1) followed by recrystallization from CH_2Cl_2/Et_2O afforded [Ru(phenq)(tpy)](PF_6)$_2$ as a red solid (38 mg, 90%): ^{1}H NMR (acetone-d_6): δ 9.35 (d, 1H, J = 9.16 Hz), 9.30 (d, 1H, J = 7.45 Hz), 9.22 (d, 1H, J = 9.16 Hz), 9.06 (d, 2H, J = 8.02 Hz), 8.73 (d, 2H, J = 8.02 Hz), 8.61 (m, 3H), 8.53 (d, 1H, J = 8.02 Hz), 8.42 (td, 2H, J = 9.16, 1.72 Hz), 8.37 (d, 1H, J = 9.16 Hz), 8.18 (t, 1H, J = 7.45 Hz), 7.97 (td, 2H, J = 6.30, 1.15 Hz), 7.82 (dd, 1H, J = 5.15, 1.15 Hz), 7.72 (d, 2H, J = 4.58 Hz), 7.66 (dd, 1H, J = 8.59, 2.86 Hz), 7.34 (dd, 1H, J = 8.02, 2.86 Hz), 7.14 (td, 2H, J = 6.87, 1.72 Hz). Anal. Calcd. for $C_{36}H_{24}N_6RuP_2F_{12} \cdot 2CH_2Cl_2$: C, 41.44; H, 2.56; N, 7.63. Found: C, 40.79; H, 1.87; N, 7.86.

Complex 9. [Ru(phenq)Cl_3] (60.0 mg, 0.12 mmol) and 4-*tert*-butyl-2,6-di([1′,8′]-naphthyrid-2′-yl)pyridine (45.6 mg, 0.12 mmol) were suspended in ethylene glycol (10 mL), and the reaction was irradiated with microwaves for 13 min (2 × 5 min, 1 × 3 min). The reaction was allowed to cool to room temperature, and NH_4PF_6 (400 mg) dissolved in water (20 mL) was added. The precipitate was filtered, washed with water, and dried. Chromatography on alumina, eluting first with CH_2Cl_2/acetone (4:1) and then with CH_2Cl_2/acetone (1:1), and recrystallization from acetone/diethyl ether afforded the product as a dark solid (28 mg, 22%): ^{1}H NMR (acetone-d_6): δ 9.53 (1H, d, J = 9.16 Hz), 9.49 (2H, s), 9.47 (1H, dd, J = 7.79, 1.37 Hz), 9.24 (1H, d, J = 8.70 Hz), 9.17 (2H, d, J = 8.24 Hz), 8.64 (2H, d, 8.70 Hz), 8.51 (1H, dd, J = 5.50, 1.37 Hz), 8.46 (1H, d, J = 8.70 Hz), 8.38 (1H, dd, J = 8.24, 0.92 Hz), 8.29–8.24 (3H, m), 8.20 (1H, dd, J = 4.35, 2.29 Hz), 8.14–8.02 (3H, m), 7.64 (1H, dd, J = 5.27, 1.37 Hz), 7.47 (1H, dd, J = 8.01, 5.04 Hz), 7.39 (2H, dd, J = 8.01, 4.12 Hz), 7.11 (1H, dd, J = 8.01, 5.04 Hz), 1.85 (9H, s). Anal. Calcd. for $C_{46}H_{34}F_{12}N_8P_2Ru \cdot 1/2H_2O$: C, 50.27; H, 3.18; N, 10.20. Found: C, 49.74; H, 2.73; N, 10.11.

X-ray Determination of 6a. All measurements were made with a Siemens SMART platform diffractometer equipped with a 4K CCD APEX II detector. A hemisphere of data (1271 frames at 6 cm detector distance) was collected using a narrow-frame algorithm with scan widths of 0.30° in omega and an exposure time of 35 s/frame. The data were integrated using the Bruker-Nonius SAINT program, with the intensities corrected for Lorentz factor, polarization, air absorption, and absorption due to variation in the path length through the detector faceplate. A psi scan absorption correction was applied based on the entire data set. Redundant reflections were averaged. Final cell constants were refined using 8156 reflections having $I > 10\sigma(I)$, and these, along with other information pertinent to data collection and refinement, are listed in Table S1, Supporting Information. The Laue symmetry was determined to be 2/m, and from the systematic absences noted the space group was shown unambiguously to be $P2_1/n$. The asymmetric unit consists of one organometallic complex, two methanols, and one solvent water molecule. One of the methanol molecules (O6) was found to be disordered over two slightly different orientations, and the minor component was modeled as an ideal rigid body. This moiety was not stable during the refinement, so finally the atomic positions were fixed in the most chemically reasonable location.

X-ray Determination of 8. All measurements were made with a Bruker DUO platform diffractometer equipped with a 4K CCD APEX II detector. A hemisphere of data (2713 frames at 4 cm detector distance) was collected using a narrow-frame algorithm with scan widths of 0.50° in omega and an exposure time of 15 s/frame. The data were integrated using the Bruker-Nonius SAINT program, with the intensities corrected for Lorentz factor, polarization, air absorption, and absorption due to variation in the path length through the detector faceplate. A psi scan absorption correction was applied based on the entire data set. Redundant reflections were averaged. Final cell constants were refined using 8093 reflections having $I > 10\sigma(I)$, and these, along with other information pertinent to data collection and refinement, are listed in Table S1, Supporting Information. The Laue symmetry was determined to be 2/m, and from the systematic absences noted the space group was shown to be $P2(1)$ or $P2(1)/m$. The refinement showed heavy disorder in almost every molecule in the asymmetric unit. One of the PF_6 anions, the acetone solvent, and the toluene solvent were found to occupy two slightly different postions, and these were treated by use of rigid body models. The main ligand of the cation was also found to be disordered such that the opposite ends exchange places. Since there was no appropriate rigid model to use due to the twisting of this moiety, distance constraints had to be used which forced homologous bonds to have essentially the same length. The two separate orientations refined to occupancies of approximately 75%:25%.

Ce(IV)-Driven Water Oxidation. A two-necked flask, fitted with a septum cap and a YSI 5331A oxygen probe connected to a YSI 5300A biological oxygen monitor, was charged with [Ce(NO_3)$_6$](NH_4)$_2$ (550 mg, 1 mmol) and water (5 mL). Before each experiment, a fresh Teflon membrane was installed over the YSI probe tip, and the probe

was calibrated in oxygen-free (N_2 purge) and oxygen-saturated (O_2 purge) water. The calibration was adjusted to give a reading of 19 ± 1% O_2 for air-saturated water. The Ce(IV) solution was purged with N_2 to provide an oxygen-free solution, and then the Ru^{II} catalyst (1×10^{-4} to 8×10^{-4} mmol) in acetonitrile (50 μL) was introduced by syringe through the septum cap. The program "Bytewedge" (Fog Software, Inc., fogsoft.com) gave an O_2 reading every 10 s for up to 30 min. The initial rates of oxygen evolution ($\mu M \cdot s^{-1}$) were calculated from the plot of oxygen evolution as a function of time. The initial rate constants (s^{-1}) were estimated from the slope of the plot of the initial rate of oxygen evolution ($\mu M \cdot s^{-1}$) as a function of the concentration of the catalyst (μM). The turnover number (TON) was determined using a GC measurement after 24 h of a reaction according to a procedure that has been previously described.[6a]

■ ASSOCIATED CONTENT

Ⓢ Supporting Information

X-ray crystallographic data for complexes **6a** and **8** in CIF format. ^1H NMR and UV−visible absorption spectra for the complexes. This material is available free of charge via the Internet at http://pubs.acs.org.

■ AUTHOR INFORMATION

Corresponding Author

*E-mail: thummel@uh.edu.

Notes

The authors declare no competing financial interest.

■ ACKNOWLEDGMENTS

We thank the Robert A. Welch Foundation (Grant E-621) and the Division of Chemical Sciences, Geosciences, and Biosciences, Office of Basic Energy Sciences of the U.S. Department of Energy (Grant DE-FG02-07ER15888) for financial support of this work. We also thank Dr. James Korp for assistance with the X-ray determinations and one of the reviewers for a helpful suggestion.

■ REFERENCES

(1) (a) Meyer, T. J. *Nature* **2008**, *451*, 778−779. (b) Holger, D.; Limberg, C.; Reier, T.; Risch, M.; Roggan, S.; Strasser, P. *ChemCatChem* **2010**, *2*, 724−761. (c) Duan, L.; Tong, L.; Xu, Y.; Sun, L. *Energy Environ. Sci.* **2011**, 3296−3313. (d) Kalyanasundaram; Graetzel, M. *Curr. Opin. Biotechnol.* **2010**, *21*, 298−310. (e) Concepcion, J. J.; Jurss, J. W.; Brennaman, M. K.; Hoertz, P. G.; Patrocinio, A. O. T.; Iha, N. Y. M.; Templeton, J. L.; Meyer, T. J. *Acc. Chem. Res.* **2009**, *42*, 1954−1965. (f) McConnell, I.; Li, G.; Brudvig, G. W. *Chem. Biol.* **2010**, *17*, 434−447. (g) Styring, S. *Faraday Discuss.* **2012**, *155*, 357−376. (h) Young, K. J.; Martini, L. A.; Milot, R. L.; Snoeberger, R. C., III; Batista, V. S.; Schmuttenmaer, C. A.; Crabtree, R. H.; Brudvig, G. W. *Coord. Chem. Rev.* **2012**, *256*, 2503−2520. (i) Yagi, M.; Syouji, A.; Yamada, S.; Komi, M.; Yamazaki, H.; Tajima, S. *Photochem. Photobiol. Sci.* **2009**, *8*, 139−147. (j) Meyer, T. J. *Acc. Chem. Res.* **1989**, *22*, 163−170.

(2) (a) Zong, R.; Thummel, R. P. *J. Am. Chem. Soc.* **2005**, *127*, 12802−12803. (b) Zhang, G.; Zong, R.; Tseng, H.-W.; Thummel, R. P. *Inorg. Chem.* **2008**, *47*, 990−998. (c) Deng, Z.; Tseng, H.-W.; Zong, R.; Wang, D.; Thummel, R. *Inorg. Chem.* **2008**, *47*, 1835−1848. (d) Kaveevivitchai, N.; Chitta, R.; Zong, R.; Ojaimi, M. E.; Thummel, R. P. *J. Am. Chem. Soc.* **2012**, *134*, 10721−10724. (e) Huang, Z.; Luo, Z.; Geletii, Y. V.; Vickers, J. W.; Yin, Q.; Wu, D.; Hou, Y.; Ding, Y.; Song, J.; Musaev, D. G.; Hill, C. G.; Lian, T. *J. Am. Chem. Soc.* **2011**, *133*, 2068−2071. (f) Blakemore, J. D.; Schley, N. D.; Balcells, D.; Hull, J. F.; Olack, G. W.; Incarvito, C. D.; Eisenstein, O.; Brudvig, G. W.; Crabtree, R. H. *J. Am. Chem. Soc.* **2010**, *132*, 16017−16029. (g) Ashford, D. L.; Stewart, D. J.; Glasson, C. R.; Binstead, R. A.; Harrison, D. P.; Norris, M. R.; Concepcion, J. J.; Fang, Z.; Templeton, J. L.; Meyer, T. J. *Inorg. Chem.* **2012**, *51*, 6428−6430. (h) Norris, M. R.; Concepcion, J. J.; Harrison, D. P.; Binstead, R. A.; Ashford, D. L.; Fang, Z.; Templeton, J. L.; Meyer, T. J. *J. Am. Chem. Soc.* **2013**, *135*, 2080−2083. (i) Li, F.; Yi, J.; Zhang, B.; Huang, F.; Gao, Y.; Sun, L. *Angew. Chem., Int. Ed.* **2012**, *51*, 2417−2420. (j) Huang, Z.; Geletii, Y. V.; Musaev, D. G.; Hill, C. L.; Lian, T. *Ind. Eng. Chem. Res.* **2012**, *51*, 11850−11859. (k) Natali, M.; Orlandi, M.; Berardi, S.; Campagna, S.; Bonchio, M.; Sartorel, A.; Scandola, F. *Inorg. Chem.* **2012**, *51*, 7324−7331. (l) Berardi, S.; Ganga, G. L.; Natali, M.; Bazzan, I.; Puntoriero, F.; Sartorel, A.; Scandola, F.; Campagna, S.; Bonchio, M. *J. Am. Chem. Soc.* **2012**, *134*, 11104−11107. (m) Wada, T.; Ohtsu, H.; Tanaka, K. *Chem.—Eur. J.* **2012**, *18*, 2374−2381.

(3) (a) Concepcion, J. J.; Jurss, J. W.; Norris, M. R.; Chen, Z.; Templeton, J. L.; Meyer, T. J. *Inorg. Chem.* **2010**, *49*, 1277−1279. (b) Wasylenko, D. J.; Ganesamoorthy, C.; Koivisto, B. D.; Henderson, M. A.; Berlinguette, C. P. *Inorg. Chem.* **2010**, *49*, 2202−2209. (c) Duan, L.; Xu, Y.; Zhang, P.; Wang, M.; Sun, L. *Inorg. Chem.* **2010**, *49*, 209−215. (d) Yoshida, M.; Masaoka, S.; Sakai, K. *Chem. Lett.* **2009**, *38*, 702−703. (e) Roeser, S.; Farràs, P.; Bozoglian, F.; Martínez-Belmonte, M.; Benet-Buchholz, J.; Llobet, A. *ChemSusChem* **2011**, *4*, 197−207. (f) Karlsson, E. A.; Lee, B.-L.; Åkermark, T.; Johnston, E. V.; Kärkäs, M. D.; Sun, J.; Hansson, Ö.; Bäckvall, J.-E.; Åkermark, B. *Angew. Chem., Int. Ed.* **2011**, *50*, 11715−11718. (g) Hull, J. F.; Balcells, D.; Blakemore, J. D.; Incarvito, D. D.; Eisenstein, O.; Brudvig, G. W.; Crabtree, R. H. *J. Am. Chem. Soc.* **2009**, *131*, 8730−8731. (h) Ellis, W. C.; McDaniel, N. D.; Bernhard, S.; Collins, T. J. *J. Am. Chem. Soc.* **2010**, *132*, 10990−10991. (i) Farràs, P.; Maji, S.; Benet-Buchholz, J.; Llobet, A. *Chem.—Eur. J.* **2013**, *19*, 7162−7172. (j) Geletii, Y. V.; Huang, Z.; Hou, Y.; Musaev, D. G.; Lian, T.; Hill, C. L. *J. Am. Chem. Soc.* **2009**, *131*, 7522−7523.

(4) (a) Yagi, M.; Tajima, S.; Komi, M.; Yamazaki, H. *Dalton Trans.* **2011**, *40*, 3802−3804. (b) Kaveevivitchai, N.; Zong, R.; Tseng, H.-W.; Chitta, R.; Thummel, R. P. *Inorg. Chem.* **2012**, *51*, 2930−2939. (c) Roeser, S.; Farràs, P.; Bozoglian, F.; Martínez-Belmonte, M.; Benet-Buchholz, J.; Llobet, A. *ChemSusChem* **2011**, *4*, 197−207. (d) Concepcion, J. J.; Jurss, J. W.; Norris, M. R.; Chen, Z.; Templeton, J. L.; Meyer, T. J. *Inorg. Chem.* **2010**, *49*, 1277−1279. (e) Concepcion, J. J.; Jurss, J. W.; Templeton, J. L.; Meyer, T. J. *J. Am. Chem. Soc.* **2008**, *130*, 16462−16463. (f) Concepcion, J. J.; Tsai, M. −K.; Muckerman, J. T.; Meyer, T. J. *J. Am. Chem. Soc.* **2010**, *132*, 1545−1557. (g) Cao, R.; Lai, W.; Du, P. *Energy Environ. Sci.* **2012**, *5*, 8134−8157. (h) Kärkäs, M. D.; Åkermark, T.; Johnston, E. V.; Karim, S. R.; Laine, T. M.; Lee, B. −L.; Åkermark, T.; Privalov, T.; Åkermark, B. *Angew. Chem., Int. Ed.* **2012**, *51*, 11589−11593. (i) Radaram, B.; Ivie, J. A.; Singh, W. M.; Grudzien, R. M.; Reibenspies, J. H.; Webster, C. E.; Zhao, X. *Inorg. Chem.* **2011**, *50*, 10564−10571.

(5) (a) Yang, X.; Hall, M. B. *J. Am. Chem. Soc.* **2009**, *132*, 120−130. (b) Yoshida, M.; Masaoka, S.; Sakai, K. *Chem. Lett.* **2009**, *38*, 702−703. (c) Masaoka, S.; Sakai, K. *Chem. Lett.* **2009**, *38*, 182−183. (d) Wasylenko, D. J.; Ganesamoorthy, C.; Koivisto, B. D.; Henderson, M. A.; Berlinguette, C. P. *Inorg. Chem.* **2010**, *49*, 2202−2209. (e) Wasylenko, D. J.; Ganesamoorthy, C.; Henderson, M. A.; Berlinguette, C. P. *Inorg. Chem.* **2011**, *50*, 3662−3672. (f) Duan, L.; Xu, Y.; Tong, L.; Sun, L. *ChemSusChem* **2011**, *4*, 238−244. (g) Kimoto, A.; Yamauchi, K.; Yoshida, M.; Masaoka, S.; Sakai, K. *Chem. Commun.* **2012**, *48*, 239−241. (h) Maji, S.; Lopez, I.; Bozohlian, F.; Benet-Buchholz, J.; Llobet, A. *Inorg. Chem.* **2013**, *52*, 3591−3593.

(6) (a) Tseng, H.-W.; Zong, R.; Muckerman, J. T.; Thummel, R. *Inorg. Chem.* **2008**, *47*, 11763−11773. (b) Zong, R.; Kaveevivitchai, N.; El Ojaimi, M.; Zhang, G.; Thummel, R. P. *Inorg. Chem.*, submitted for publication.

(7) Tong, L.; Duan, L.; Xu, Y.; Privalov, T.; Sun, L. *Angew. Chem., Int. Ed.* **2011**, *50*, 445−449.

(8) Duan, L.; Fischer, A.; Xu, Y.; Sun, L. *J. Am. Chem. Soc.* **2009**, *131*, 10397−10399.

(9) Medlycott, E. A.; Hanan, G. S. *Chem. Soc. Rev.* **2005**, *34*, 133−142.

(10) Abrahamsson, M.; Becker, H.-C.; Hammarstrom, L.; Bonnefous, C.; Chamchoumis, C.; Thummel, R. P. *Inorg. Chem.* **2007**, *46*, 10354−10364.
(11) De Cian, A.; DeLemos, E.; Mergny, J.-L.; Teulade-Fichou, M.-P.; Monchaud, D. *J. Am. Chem. Soc.* **2007**, *129*, 1856−1857.
(12) Sullivan, B. P.; Calvert, J. M.; Meyer, T. J. *Inorg. Chem.* **1980**, *19*, 1404−1407.
(13) Hu, Y.-Z.; Wilson, M. H.; Zong, R.; Bonnefous, C.; McMillin, D. R.; Thummel, R. P. *Dalton Trans.* **2005**, 354−358.